

BP-ANN for Fitting the Temperature-Germination Model and Its Application in Predicting Sowing Time and Region for Bermudagrass

Erxu Pi¹, Nitin Mantri³, Sai Ming Ngai⁴, Hongfei Lu^{2*}, Liqun Du^{1*}

1 College of Life and Environmental Science, Hangzhou Normal University, Hangzhou, Zhejiang, PR China, **2** College of Life Science, Zhejiang Sci-Tech University, Hangzhou, Zhejiang, PR China, **3** School of Applied Sciences, Health Innovations Research Institute, RMIT University, Melbourne, Victoria, Australia, **4** Department of Biology, The Chinese University of Hong Kong, Shatin, Hong Kong SAR

Abstract

Temperature is one of the most significant environmental factors that affects germination of grass seeds. Reliable prediction of the optimal temperature for seed germination is crucial for determining the suitable regions and favorable sowing timing for turf grass cultivation. In this study, a back-propagation-artificial-neural-network-aided dual quintic equation (BP-ANN-QE) model was developed to improve the prediction of the optimal temperature for seed germination. This BP-ANN-QE model was used to determine optimal sowing times and suitable regions for three *Cynodon dactylon* cultivars (*C. dactylon*, 'Savannah' and 'Princess VII'). Prediction of the optimal temperature for these seeds was based on comprehensive germination tests using 36 day/night (high/low) temperature regimes (both ranging from 5/5 to 40/40°C with 5°C increments). Seed germination data from these temperature regimes were used to construct temperature-germination correlation models for estimating germination percentage with confidence intervals. Our tests revealed that the optimal high/low temperature regimes required for all the three bermudagrass cultivars are 30/5, 30/10, 35/5, 35/10, 35/15, 35/20, 40/15 and 40/20°C; constant temperatures ranging from 5 to 40°C inhibited the germination of all three cultivars. While comparing different simulating methods, including DQEM, Bisquare ANN-QE, and BP-ANN-QE in establishing temperature based germination percentage rules, we found that the R^2 values of germination prediction function could be significantly improved from about 0.6940–0.8177 (DQEM approach) to 0.9439–0.9813 (BP-ANN-QE). These results indicated that our BP-ANN-QE model has better performance than the rests of the compared models. Furthermore, data of the national temperature grids generated from monthly-average temperature for 25 years were fit into these functions and we were able to map the germination percentage of these *C. dactylon* cultivars in the national scale of China, and suggested the optimum sowing regions and times for them.

Citation: Pi E, Mantri N, Ngai SM, Lu H, Du L (2013) BP-ANN for Fitting the Temperature-Germination Model and Its Application in Predicting Sowing Time and Region for Bermudagrass. PLoS ONE 8(12): e82413. doi:10.1371/journal.pone.0082413

Editor: Joshua L. Heazlewood, Lawrence Berkeley National Laboratory, United States of America

Received: June 5, 2013; **Accepted:** November 1, 2013; **Published:** December 13, 2013

Copyright: © 2013 Pi et al. This is an open-access article distributed under the terms of the Creative Commons Attribution License, which permits unrestricted use, distribution, and reproduction in any medium, provided the original author and source are credited.

Funding: This work was supported by grant U1130304 and 31301053 from National Science Foundation of China, and the Technology Research and Development Program of Jiangsu Province (BE2012416) and Six Key Talents Program of Jiangsu (2011NY032). No additional external funding received for this study. The funder had no role in study design, data collection and analysis, decision to publish, or preparation of the manuscript.

Competing Interests: The authors have declared that no competing interests exist.

* E-mail: luhongfei63@yahoo.com.cn (HL); liqundu@hznu.edu.cn (LD)

Introduction

Cynodon dactylon (Linnaeus) Persoon (Family: Poaceae, bermudagrass in English) is a perennial, creeping grass. Although it is widely found in the tropical and warm temperate regions, bermudagrass is predominantly distributed between 45° North and 45° South latitudes [1,2]. Currently, *C. dactylon* is globally used as a turf grass, fodder and medicinal plant, and it was also used for removal of heavy metals from contaminated soils [3–5]. This grass is adapted to extremely variable environments, such as fertile fields, arid land, saline land, wet irrigation canals and even contaminated wastelands with high levels of Pb, Cd, Zn and Cu [6–10]. In addition, the extracts from bermudagrass are well known for various medicinal properties including antimicrobial [11,12], anti-inflammatory [13,14], immunomodulatory [15,16] and anti-diarrhea activities [17]. It has been therefore used to treat traumatic wounding, kidney calculi [18], hypoglycemia [19], depression [20] and cancer [21–23].

Seed germination percentage is a major criterion used for evaluating suitability of an environment for grass cultivation. Previous studies showed that extreme temperatures could lead to seed dormancy and significantly decreased germination percentage [24–26]. Constructing a precise mathematical model that correlates the germination percentage with temperature may avoid failure of plantation due to inappropriate sowing timing or mismatch between the grass species and climate zone. Hence it would be very helpful for decision-makers to select grass species and sowing time for lawn, erosion control and forage cultivation. Using thermal time approach, Bradford [27] constructed temperature/water potential based seed germination and dormancy models. This study showed that germination experiments under temperature regime with discrete (stepwise) changes could also be used to accurately predict thermal responses of seeds in field environment with continuously changing temperature. Hardegree and Van Vactor [28,29] used the Piece-wise linear (PWL) regression equations to confirm that constant-temperature

experimental results derived mathematical models could be used to predict the germination/growth responses to the combined effects of multiple environmental factors in the field. Although various experimental procedures have been established to generate data for the development and validation of reliable prediction models [30–35], the R^2 values of temperature-germination percentage functions in some of the previous studies were relatively low (0.61–0.80) [34,36] and more accurate predictions are desired.

Recently, the Geographic Information System (GIS) based spatial prediction approach was introduced for the creation of quantitative and accurate grass suitability maps [36]. The grid data of mean minimum and maximum temperatures [37] were used for calculating suitability values of regions *via* the temperature-germination percentage functions. Therefore, the suitability of grass for different regions could be appropriately visualized on the map. However, the visualization of time scale (season) of these maps remains to be streamlined for readability to facilitate their practical application.

The objectives of this research were to: (i) explain the correlation error between temperature and seed germination percentage caused by selection of functions (ii) provide a new program for optimizing the temperature-germination function, (iii) use temperature-based seed germination percentage function in combination with national temperature grids in China for predicting the suitability of three bermudagrass cultivars, *C. dactylon*, ‘Savannah’ and ‘Princess VII’.

Results

Germination response to Diurnal Fluctuations of Temperature

The germination response of the three bermudagrass cultivars was similar (Tables 1–3). All the three cultivars were capable of germinating in warm-period temperature (T_2) from 25 to 35°C and cool-period temperature (T_1) ranging from 5–40°C. The optimal temperature for seed germination is defined as that which is not lower than the maximum germination minus one-half of its confidence interval ($P=0.05$). For example, the maximum

germination percentage (the optimal temperature for seed germination) of *C. dactylon* was 87.3% at 15/35°C (Table 1); and the germination percentage at 5/30°C was only 80.7%, but it was still accepted as the optimal temperature for seed germination since the one-half of its confidence interval was 7.0% and 80.7% > (87.3%–7.0%). Fluctuating between 5–25°C cool-period temperature and 30–40°C warm-period temperature gave rise to the optimal temperature for seed germination. On the other hand, germination percentage was usually lower than 50% at constant temperature ranging from 20 to 40°C (except the ‘Savannah’ at constant 25/25°C in Table 2), for example the germination percentages of ‘Princess VII’ (Table 1), were 0, 36.0%, 5.3%, 12.7% and 20.0% at constant temperature regimes of 20/20, 25/25, 30/30, 35/35 and 40/40°C, respectively. Interestingly, germination percentage of *C. dactylon* seed at a constant 30°C only reached 1.3%.

The maximum germination and the mean of germination of the three bermudagrass cultivars are presented in Table 4. The germination percentage of ‘Princess III’ appeared to be the highest (96.7%), but it was not significantly different ($P>0.05$) from that of the other two cultivars (87.3% and 94.0% for *C. dactylon* and ‘Savannah’, respectively). Depending on the cultivar, 25%–27.8% of the temperature regimes supported the optimal temperature for seed germination. Only eight temperature regimes, 30/5, 30/10, 35/5, 35/10, 35/15, 35/20, 40/15 and 20/40°C, supported the optimal temperature for seed germination for all three tested cultivars (Tables 1–4).

Performance of Different Regression Models

All the regression equations of temperature treatments that assess the germination suitability of the three bermudagrass cultivars are summarized in Table 5. Quadratic and quintic general equations were used for data simulation. The bisquare and BP-ANN approaches (Fig. 1) were utilized for optimizing these equation coefficients. There was no significant difference between the quintic functions and bisquare optimized quintic functions. Bisquare quintic functions of cultivars *C. dactylon*, ‘Savannah’ and ‘Princess VII’ showed lower R^2 than quintic functions (data not

Table 1. Quadratic response surface based on estimated percent germination with confidence interval at the 0.05 probability level for seeds of the *C. dactylon*.

Cool period temperature (°C) 16 h	Warm period temperature (°C) 8 h							
	5	10	15	20	25	30	35	40
	% Germination after 15–20 days							
5	0.0±0.0	0.0±0.0	0.0±0.0	0.0±0.0	28.0±7.2	80.7±7.0*	76.7±9.5*	21.3±4.2
10		0.0±0.0	0.0±0.0	0.0±0.0	36.7±3.1	82.7±8.1*	84.7±5.0*	42.0±6.9
15			0.0±0.0	0.0±0.0	44.0±4.0	82.0±3.5*	[87.3±8.3]	79.3±3.1*
20				0.0±0.0	4.7±1.2	59.3±8.1	79.3±7.0*	81.3±13.3*
25					4.7±1.2	5.3±1.2	52.7±8.1	58.7±5.0
30						1.3±1.2	1.3±1.2	7.3±3.1
35							5.3±3.1	13.3±5.0
40								3.3±2.3

*Note: 1. Data presented are mean ± a half of the confidence interval as determined from regression equations. The maximum calculated germination is enclosed by brackets.

2. Means not lower than the maximum germination minus one-half of its confidence interval.

doi:10.1371/journal.pone.0082413.t001

Table 2. Quadratic response surface based on estimated percent germination with the confidence interval at the 0.05 probability level for seeds of the cultivar ‘Savannah’.

Cool period temperature (°C) 16 h	Warm period temperature (°C) 8 h							
	5	10	15	20	25	30	35	40
	% Germination after 15–20 days							
5	0.0±0.0	0.0±0.0	0.0±0.0	24.7.0±4.2	77.3±6.1	86.0±5.3*	91.3±2.3*	82.7±13.3*
10		0.0±0.0	0.0±0.0	34.7.0±3.1	83.3±4.2	88.0±3.5*	88.7±2.3*	80.7±3.1
15			0.0±0.0	33.3.0±4.6	83.3±3.1	71.3±4.2	92.7±1.2*	87.3±6.4*
20				13.7.0±6.4	46.0±9.2	81.3±4.2	83.3±11.4*	[94.0±3.5]
25					61.3±4.2	42.0±13.1	73.3±4.6	91.3±4.6*
30						36.7±7.0	66.0±5.3	40.0±3.5
35							49.3±8.3	60.0±4.0
40								35.3±5.0
5	0.0±0.0	0.0±0.0	0.0±0.0	24.7.0±4.2	77.3±6.1	86.0±5.3*	91.3±2.3*	82.7±13.3*

*Note: 1. Data presented are mean ± a half of the confidence interval as determined from regression equations. The maximum calculated germination is enclosed by brackets.
 2. Means not lower than the maximum germination minus one-half of its confidence interval.
 doi:10.1371/journal.pone.0082413.t002

shown). Similar optimization results were observed for all the cultivars tested. Generally, quintic equations performed better than quadratic equations (Fig. 2, Table 5). The highest R² values were generated by the back propagation artificial neural networks aided dual quintic equation (BP-ANN-QE) model (0.9439 to 0.9813). In contrast, the dual quadratic equation model (DQEM) generated the lowest R² values (0.6940 to 0.8177).

Contour plot maps were then used to visualize the prediction errors generated from different simulation functions (Fig. 2). The blue spot represents the experimental germination percentage associated with particular fluctuating temperature combinations. Obviously, DQEM is the one most prone to produce prediction errors among the compared models (Fig. 2A, D and G). However, some weakness in functional convergence of quintic equations was

observed, a small portion of observed temperature-germination spots were still out of their equation derived surfaces (Fig. 2B, C, E, F, H and I).

Spatial Mapping of Optimal Planting Times

The temperature-germination functions derived from our experimental data were used to predict germination percentage for various regions in China in different seasons using the 25 years mean minimum and mean maximum earth surface temperature grids as input. The percentage reflected the likelihood of germination suitability at each grid cell of the maps *via* FreeMicaps (Fig. 3–5). The results reveal that most of the Chinese regions are not suitable for seed germination of all the tested bermudagrass cultivars from November to March. Although ‘Savannah’ has the

Table 3. Quadratic response surface based on estimated percent germination with the confidence interval at the 0.05 probability level for seeds of the cultivar ‘Princess VII’.

Cool period temperature (°C) 16 h	Warm period temperature (°C) 8 h							
	% Germination after 15–20 days							
	5	10	15	20	25	30	35	40
5	0.0±0.0	0.0±0.0	0.0±0.0	0.0±0.0	54.7±1.2	91.3±2.3*	96.0±3.5*	66.0±13.1
10		0.0±0.0	0.0±0.0	0.0±0.0	76.7±4.6	[96.7±2.3]	95.3±1.2*	49.3±6.4
15			0.0±0.0	0.0±0.0	83.3±3.1	94.0±2.0*	94.7±1.2*	94.0±3.5*
20				0.0±0.0	16.0±2.0	84.7±7.0	[96.7±11.4]	92.7±3.1*
25					36.0±2.0	18.7±8.3	86.7±6.4	90.0±5.3*
30						5.3±5.8	18.0±2.0	16.0±12.5
35							12.7±5.8	34.7±6.1
40								20.0±7.2

*Note: 1. Data presented are mean ± a half of the confidence interval as determined from regression equations. The maximum calculated germination is enclosed by brackets.
 2. Means not lower than the maximum germination minus one-half of its confidence interval.
 doi:10.1371/journal.pone.0082413.t003

Table 4. Comparison of the temperature-germination profiles for the five bluegrass cultivars.

Germination parameter	Sources		
	<i>C. dactylon</i>	Savannah	Princess VII
Profile mean	31.3	52.7	45.0
Regimes with some germination	72.2	83.3	72.2
Maximum germination	87.3	94.0	96.7
Mean of some germination*	43.3	63.2	62.3
Mean of optima	81.6	88.5	94.1
Regimes with optimum germination	25.0	27.8	27.8
Profile mean	31.3	52.7	45.0

Note: *The mean of some germination refers to the mean value of regimes with any germination more than zero [47,52].
doi:10.1371/journal.pone.0082413.t004

narrowest geographic range of germination with percentages arranging from above 0 to 100%, it was predicted to have optimal temperatures for germination in widest geographic range in China (Fig. 4). In contrast, *C. dactylon* had the narrowest range for the optimal temperatures for seed germination (Fig. 3). For both *C. dactylon* and ‘Princess VII’, the widest range with the optimal temperatures for seed germination was in the month of June, whilst for ‘Savannah’ it was in May (Fig. 3–5).

Discussion

Simulation models have been widely used to correlate cultivation conditions and plant germination/growth [38–40]. These regression models were generally used to predict the plant suitability to particular regions where climate and soil environment information is available. These mathematical models could help grass cultivation in three major aspects. First, these functions combined with a visual suitability map may help decision makers in selecting a grass species and planning its seeding timing [36,41]. Second, they may serve as useful tools for identifying and evaluating desirable quantitative characteristics for specific grass breeding objectives [42], which is helpful in coupling genotype and phenotype of a target cultivar, a technology with significant application value in the rapidly expanding turf industry [43]. Third, these grass-condition models may improve our understanding of how changes in agricultural systems would quantitatively influence grass germination/growth [44].

Comparison of Regressions Using Quadratic and Quintic Equations

The quadratic equation was broadly accepted as an effective statistical tool for simulating continuous variable-response relationship, and quadratic response surface has been a predominant method to analyze germination performance of grass seeds under various temperature regimes, especially to test the seed germination affected by diurnal temperature treatments [36,41]. However, the weakness of quadratic equation is also obvious. Since the two-dimensional quadratic response surface cannot display some errors in the global fitting between quadratic function and experimental data [36], the weakness of low R^2 values (0.61–0.80) was ignored. In this study, quintic equation was employed for regression to

simulate diurnal temperature-germination responses of three bermudagrass cultivars. Compared to quadratic surfaces, quintic approaches had significantly lower fitting errors and higher confidence (Fig. 2 and Table 5). This may be due to the nonlinear temperature-germination correlation. Hence these quintic equation models could provide more reliable predictions for field performance of grasses, further improving the reliability of the suitability map of grasses tinted with different color based on predicted germination percentage data.

BP-ANN and Bisquare for Intercept and Coefficients Fitting

Artificial Neural Network (ANN), an algorithm for simulating the thinking processes of the human brain which usually have multiple networks that are logically arranged as fundamental units [45]. The information of any unit can be learnt, recalled, concluded and speculated. Hence, the ANN has many advantages such as distributed storage of information, self-adaptability, self-organization and fault-tolerance properties [40]. As a computer based program, it could be used to perform large-scale parallel calculations to simulate nonlinear correlation [46]. Therefore, ANN is broadly used in various of fields including biomedical research [47,48], optimization of soil nutrient distribution coefficient [43,49,50], forecasting of microorganism community assemblages [51], prediction of animal metabolism and diets correlation [52], and simulation of fruit post-ripening process [53–55].

Currently, there are tens of ANN models. Amongst them, the back propagation (BP) network is the most widely used one for simulation of nonlinear relationship [56]. The BP-ANN model belongs to supervised study and its training process has two phases, forward propagation and backward propagation [57]. In the forward propagation, the weighted value and threshold value of each layer is calculated by iteration and passed into the BP three-layer network. Subsequently, the backward propagation uses the weighted value and threshold values for revision [58]. These two phases commonly occur repeatedly for about 10,000 times, and the weighted value and threshold values alternate until they converge. The target of these training processes is to generate a function that can globally ‘distinguish’ and ‘remember’ all the input raw data [59]. Therefore, the simulated BP-ANN functions could be used to predict proposed parameter with appropriate input variables.

The robust bisquare estimator, also known as Tukey’s bi-weight function, was a popular choice for nonlinear function fitting [60]. This estimator was often used for smoothing the nonlinear response surface [61,62]. It was reported that bisquare estimator could be adapted to process noisy data with outliers [63].

In our study, both BP-ANN and bisquare methods were used to optimize the temperature-germination functions for three bermudagrass cultivars. We did not find significant difference between general quintic functions and bisquare fitted quintic functions. Furthermore, most bisquare quintic functions in this study had slightly lower R^2 values than the quintic functions. Therefore, the BP-ANN optimized quintic equations were found to be the best option for fitting temperature-germination functions of the tested bermudagrass cultivars.

To some degree, the BP-ANN based temperature-germination functions could be evaluated by the visualized suitability map (Figs. 3–5) and the observed temperature-germination results (Tables 1–3). Generally, the cultivar ‘Savannah’ could germinate under the widest temperature regimes (Tables 1–3), from about 20/5°C to 40/40°C, it also present the highest suitability with widest geographic regions in China (eg. Fig. 4D–I). On the other

Table 5. Equations and R² values for predicting germination as a function of cool (T₁) and warm (T₂) temperature treatments for the three *C. dactylon* cultivars tested.

Cultivars		R ²	Equation
<i>C. dactylon</i>	Quadratic	0.8177	$Y = -0.5856 + 0.06925 * T_1 - 0.006143 * T_2 - 0.0008586 * T_1^2 + 0.0006574 * T_1 * T_2 - 0.0007847 * T_2^2$
	Quintic+Bisquare	0.9166	$Y = 0.4026 + 0.02444 * T_1 - 0.133 * T_2 - 0.0291 * T_1^2 + 0.05145 * T_1 * T_2 - 0.01535 * T_2^2 + 0.002361 * T_1^3 - 0.002139 * T_1^2 * T_2 - 0.002076 * T_1 * T_2^2 + 0.001802 * T_2^3 - 6.199e-005 * T_1^4 - 7.613e-006 * T_1^3 * T_2 + 0.0002068 * T_1^2 * T_2^2 - 0.0001705 * T_1 * T_2^3 + 2.974e-005 * T_2^4 + 5.357e-007 * T_1^5 + 5.886e-007 * T_1^4 * T_2 - 2.712e-006 * T_1^3 * T_2^2 + 1.219e-006 * T_1^2 * T_2^3 + 1.018e-006 * T_1 * T_2^4 - 5.966e-007 * T_2^5$
	Quintic+BP-ANN	0.9813	$Y = -0.2789 + 15.74 * T_1 - 11.43 * T_2 - 88.16 * T_1^2 + 31.27 * T_1 * T_2 + 34.83 * T_2^2 + 180.4 * T_1^3 + 0.5264 * T_1^2 * T_2 - 128.8 * T_1 * T_2^2 - 3.322 * T_2^3 - 139 * T_1^4 - 163.4 * T_1^3 * T_2 + 510.2 * T_1^2 * T_2^2 - 462.2 * T_1 * T_2^3 + 206.5 * T_2^4 + 32.55 * T_1^5 + 124.5 * T_1^4 * T_2 - 312.5 * T_1^3 * T_2^2 + 248.7 * T_1^2 * T_2^3 - 16.93 * T_1 * T_2^4 - 59.17 * T_2^5$
Savannah	Quadratic	0.7617	$Y = -0.5168 + 0.06924 * T_1 - 0.01989 * T_2 - 0.000934 * T_1^2 + 0.001138 * T_1 * T_2 - 0.0007981 * T_2^2$
	Quintic+Bisquare	0.9301	$Y = 0.3523 + 0.04868 * T_1 - 0.1349 * T_2 - 0.0311 * T_1^2 + 0.04712 * T_1 * T_2 - 0.01236 * T_2^2 + 0.002363 * T_1^3 - 0.001472 * T_1^2 * T_2 - 0.002595 * T_1 * T_2^2 + 0.001872 * T_2^3 - 6.187e-005 * T_1^4 - 9.422e-006 * T_1^3 * T_2 + 0.0001502 * T_1^2 * T_2^2 - 7.953e-005 * T_1 * T_2^3 - 9.526e-006 * T_2^4 + 5.348e-007 * T_1^5 + 5.833e-007 * T_1^4 * T_2 - 2.575e-006 * T_1^3 * T_2^2 + 2.423e-006 * T_1^2 * T_2^3 - 1.543e-006 * T_1 * T_2^4 + 7.051e-007 * T_2^5$
	Quintic+BP-ANN	0.9507	$Y = -0.1454 + 6.803 * T_1 - 3.249 * T_2 - 67.57 * T_1^2 + 66.13 * T_1 * T_2 - 26.76 * T_2^2 + 192.9 * T_1^3 - 132.7 * T_1^2 * T_2 - 75.01 * T_1 * T_2^2 + 99.66 * T_2^3 - 198.7 * T_1^4 - 14.87 * T_1^3 * T_2 + 537.8 * T_1^2 * T_2^2 - 577.8 * T_1 * T_2^3 + 155 * T_2^4 + 67.97 * T_1^5 + 78.26 * T_1^4 * T_2 - 403.7 * T_1^3 * T_2^2 + 414.8 * T_1^2 * T_2^3 - 104.4 * T_1 * T_2^4 - 13.94 * T_2^5$
Princess VII	Quadratic	0.6940	$Y = -0.5152 + 0.0604 * T_1 - 0.01284 * T_2 - 0.0008349 * T_1^2 + 0.001594 * T_1 * T_2 - 0.001628 * T_2^2$
	Quintic+Bisquare	0.9191	$Y = -0.4047 + 0.5009 * T_1 - 0.3331 * T_2 - 0.08726 * T_1^2 + 0.06563 * T_1 * T_2 - 0.002549 * T_2^2 + 0.004956 * T_1^3 - 0.001118 * T_1^2 * T_2 - 0.00565 * T_1 * T_2^2 + 0.003324 * T_2^3 - 0.0001053 * T_1^4 - 0.0001238 * T_1^3 * T_2 + 0.0005272 * T_1^2 * T_2^2 - 0.000455 * T_1 * T_2^3 + 0.0001159 * T_2^4 + 7.324e-007 * T_1^5 + 2.591e-006 * T_1^4 * T_2 - 8.149e-006 * T_1^3 * T_2^2 + 6.436e-006 * T_1^2 * T_2^3 - 4.407e-007 * T_1 * T_2^4 - 7.708e-007 * T_2^5$
	Quintic+BP-ANN	0.9439	$Y = -0.6384 + 24.43 * T_1 - 13.54 * T_2 - 155.9 * T_1^2 + 87.77 * T_1 * T_2 + 6.161 * T_2^2 + 356.5 * T_1^3 - 117 * T_1^2 * T_2 - 165.9 * T_1 * T_2^2 + 75.58 * T_2^3 - 322.3 * T_1^4 - 109.2 * T_1^3 * T_2 + 725.6 * T_1^2 * T_2^2 - 663.2 * T_1 * T_2^3 + 212.7 * T_2^4 + 99.58 * T_1^5 + 134.6 * T_1^4 * T_2 - 482.2 * T_1^3 * T_2^2 + 432.9 * T_1^2 * T_2^3 - 94.28 * T_1 * T_2^4 - 31.4 * T_2^5$

doi:10.1371/journal.pone.0082413.t005

hand, the predicted suitability map worked in concert with the observations that all the three cultivars preferred warm temperature above 15/15°C (Tables 1–3), and little germination could be found during the cool seasons in China (eg. Fig. 4A–C).

Conclusions

This study tested the influence of diurnal fluctuations of temperatures on seed germination of three bermudagrass cultivars (*C. dactylon*, ‘Savannah’ and ‘Princess VII’). Eight temperature regimes, 5/30, 10/30, 5/35, 10/35, 15/35, 20/35, 15/40 and 20/40°C, supported the optimal temperature for seed germination for the three cultivars. However, the germination percentage of all the three cultivars was lower than 50% under conditions of constant temperatures ranging from 5 to 40°C.

To simulate the grass germination-temperature response function, both quadratic and quintic equations were employed. Quintic functions performed significantly better (R² were around 0.9439) than the quadratic ones (R² ranging from 0.6940~0.8177) for the tested cultivars. The main objective of this study was to test the nonlinear fitting approaches, bisquare and BP-ANN, for optimizing the regression functions. Our results suggested that BP-ANN has significant advantages over bisquare for fitting the intercept and coefficients of the temperature-germination functions.

Based on the experimentally derived BP-ANN functions and available climate data, we prepared a seed suitability map of three bermudagrass cultivars for cultivation in the People’s Republic of China. We observed that most of the regions in China are not suitable for bermudagrass seed germination from November to

March. The cultivar ‘Savannah’ had the widest geographic range of the optimal temperature for seed germination, whilst *C. dactylon* had the narrowest range of the optimal temperature for seed germination percentage. The month with widest range of the optimal temperature for seed germination for *C. dactylon* and ‘Princess VII’ is June, whilst for ‘Savannah’, it is May.

Materials and Methods

Seeds and Conditioning

The bermudagrass cultivars (*C. dactylon*, ‘Savannah’ and ‘Princess VII’) were planted widely in China. All the grass seeds were purchased from Shanghai Chunyin Turf Inc., (Shanghai, China) and stored at room temperature until use. Seed viability was tested on sterilized wet filter paper at 25°C in darkness [36].

Briefly, seeds were surface sterilized in 0.01% HgCl₂ for 1 min followed by four rinses with distilled water. The seeds were subsequently placed on wet filter papers in Petri dishes. The Petri dishes were placed in incubators set up for 36 different regimes of diurnal fluctuations of temperature treatments: 16 h at temperature T₁ and 8 h at temperature T₂. The T₁ and T₂ ranged from 5 to 40°C with 5°C increments [36]. Germinated seeds were counted daily until no further germination occurred (about 15–20 days) for viability analysis (Supplementary file Tables 1–3). For each experiment, three replications of 50 seeds were used in a randomized block design.

Statistical Analysis

In this study, quadratic and quintic response surfaces were constructed with estimated means and confidence intervals [64].

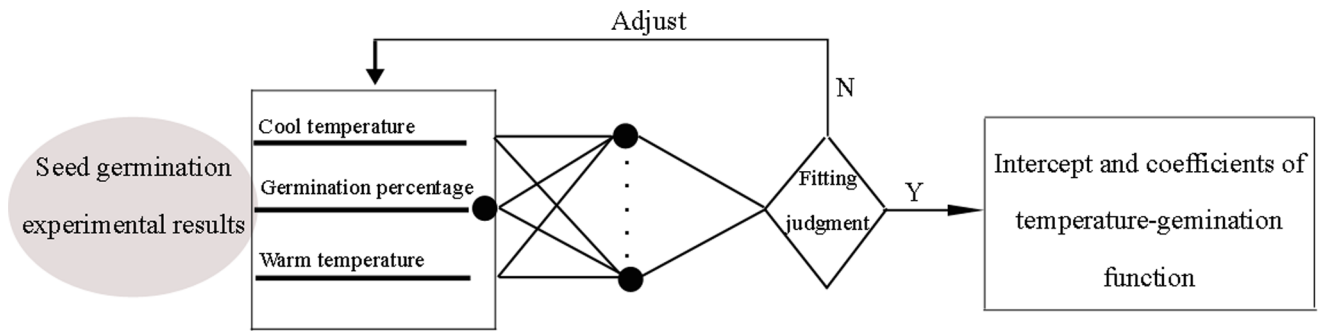


Figure 1. Schematic diagram of back propagation artificial neural networks used for fitting the regression functions of bermudagrass germination response to diurnal fluctuations of temperature.
doi:10.1371/journal.pone.0082413.g001

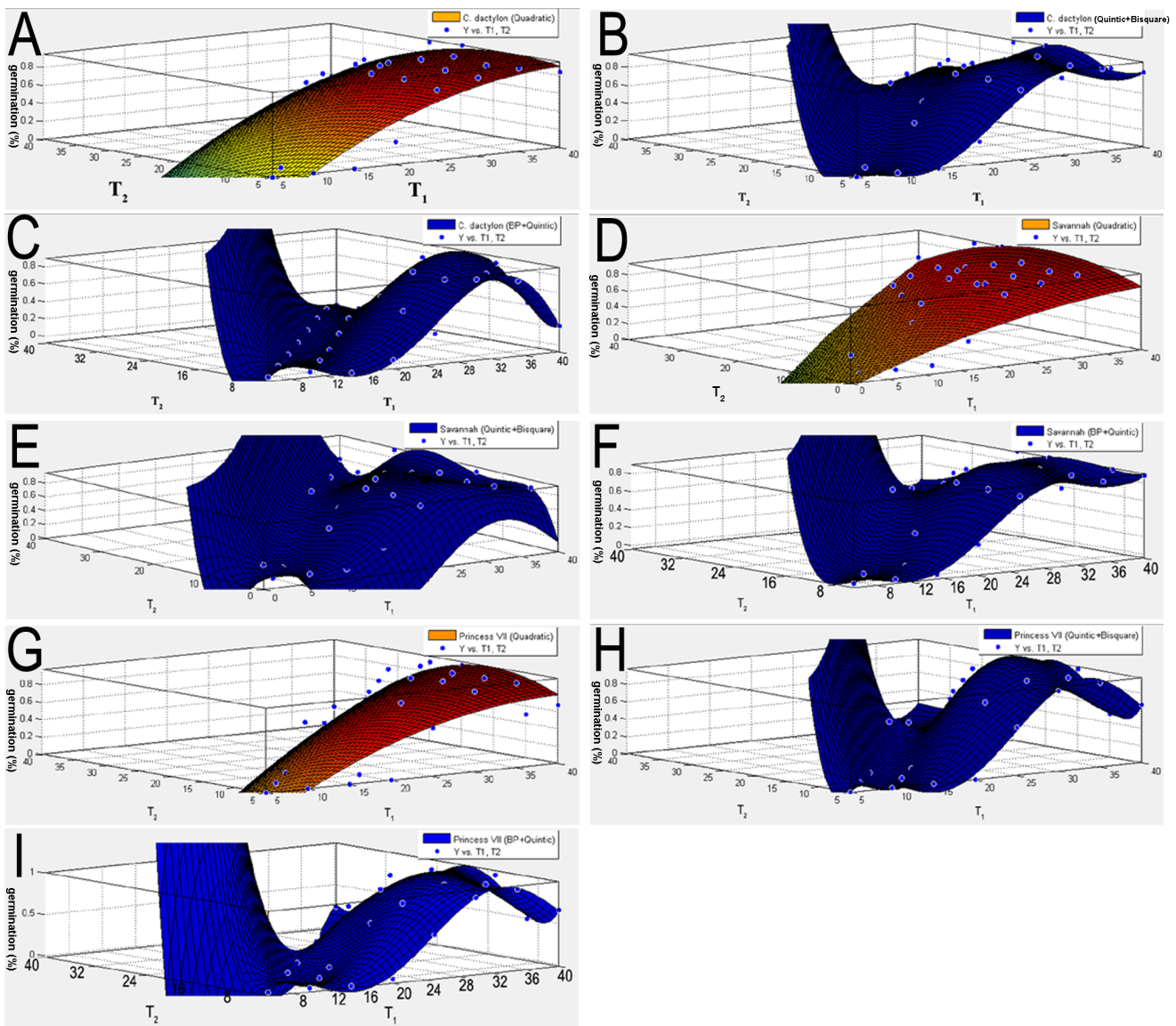


Figure 2. Three dimensional plot map of bermudagrass germination in which the estimated percent germination values in different temperature regimes were used for their constructions; (A–C) *C. dactylon*, (D–F) ‘Savannah’ and (G–I) ‘Princess VII’.
doi:10.1371/journal.pone.0082413.g002

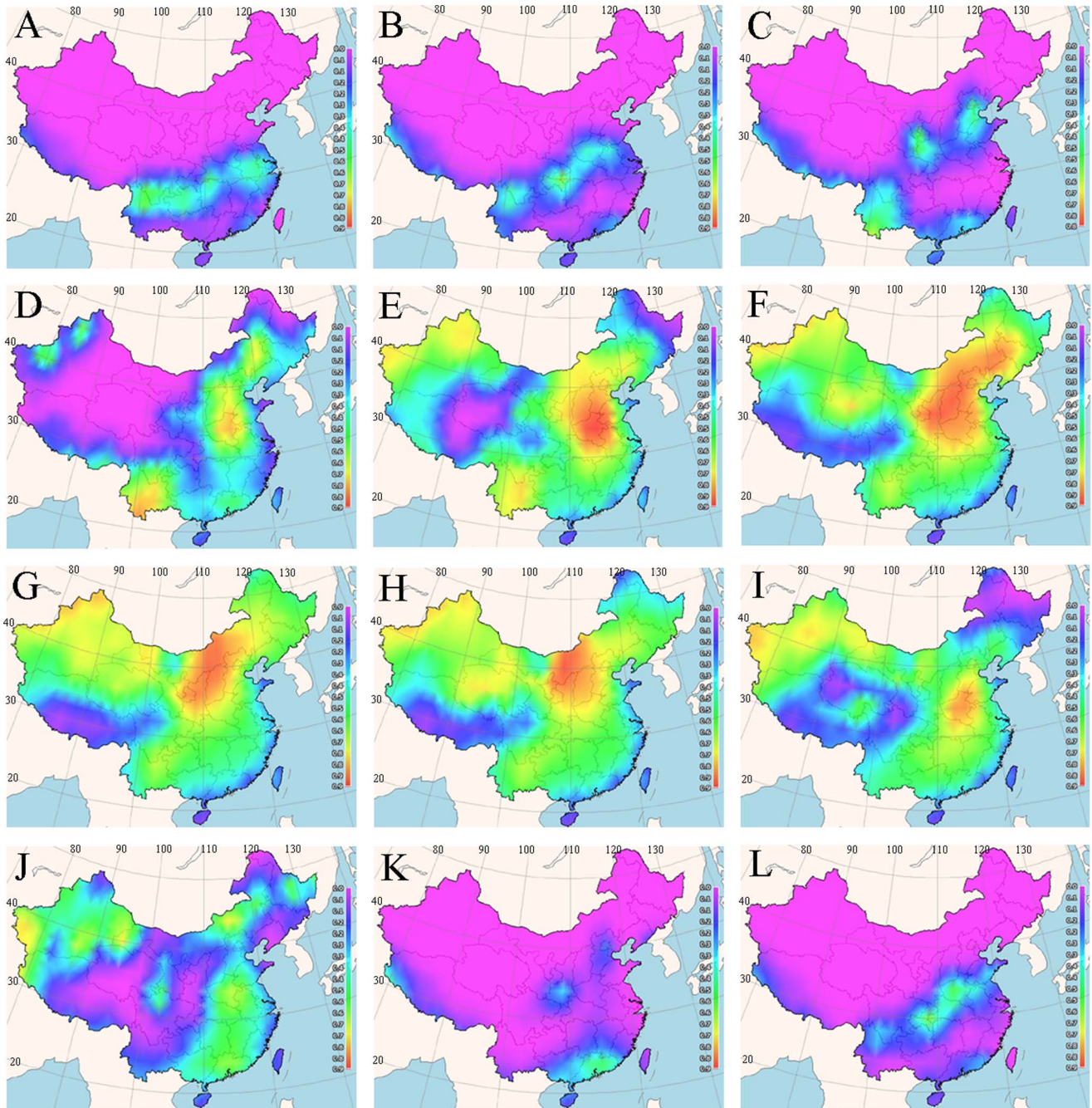


Figure 3. Maps of monthly germination suitability for *C. dactylon* in different regions of China; (A-L) January-December.
doi:10.1371/journal.pone.0082413.g003

The quadratic equations were first used for estimating germination percentages. The generalized equation was [36]:

$$Y_1 = A_0 + A_1 * T_1 + A_2 * T_2 + A_3 * T_1^2 + A_4 * T_2^2 + A_5 * T_1 * T_2,$$

where Y_1 : predicted germination percentage, A_0 : intercept, A_1 through A_5 : coefficients, T_1 and T_2 : two temperature in the diurnal regime.

Meanwhile, quintic equations with the following generalized equation were also used to simulate the temperature-germination function: $Y_1 = \sum_{m=1}^5 \left\{ \sum_{n=0}^m [T_1^n * T_2^{m-n}] * f(A) \right\} + A_0'$, where A_0' : intercept, $f(A)$: coefficient function. Temperature inputs were normalized by dividing the maximum value. Subsequently, the intercept and coefficients were optimized using Bisquare, a default curve fitting method of MATLAB 7.9-R2009b software and back propagation artificial neural networks (BP-ANN) approach described in Fig. 1, respectively. The BP-ANN (or feed-forward network) has the capability to learn arbitrary nonlinearity and

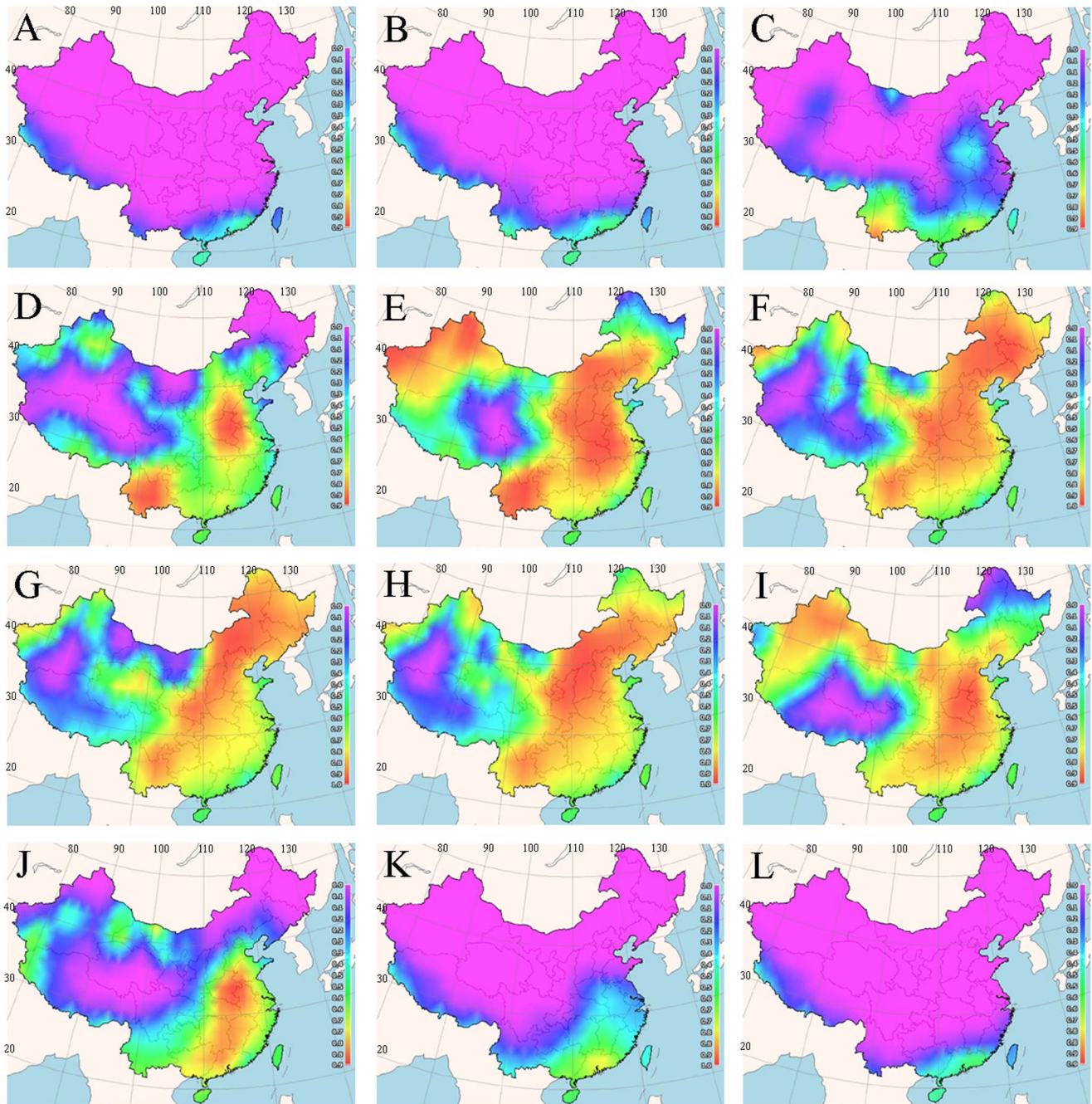


Figure 4. Maps of monthly germination suitability for 'Savannah' in different regions of China; (A–L) January–December.
doi:10.1371/journal.pone.0082413.g004

great potential for adaptive control applications [46]. In the BP-ANN, the correlations among the input variables do not need to be specified. Instead, they learn from the examples fed to them (Fig. 1). In addition, they can generalize correct responses that only broadly resemble the data in the learning phase [56,65,66].

Spatial Mapping

The suitability of a grass is represented by seed germination percentage. The grass suitability maps were created using the FreeMicaps software (<http://bbs.121323.com/guojif/FreeMicaps20111001.rar>). Like the Surfer software [67], FreeMicaps also uses grid data at selected points (station) that is

compatible with GIS. The temperature data of adjacent regions around the station are generated using regression functions. The data used to construct the temperature grid are curated in the database in National Aeronautics and Space Administration (NASA, <http://power.larc.nasa.gov/cgi-bin/cgiwrap/solar/sse.cgi?grid@larc.nasa.gov#s11>) which are composed of minimum and maximum daily temperature of earth surface from 313 Chinese weather stations for a period of 25 years (from 1983 to 2007). These mean values of minimum and maximum daily temperatures were used as the T_1 and T_2 variables, respectively in the BP-ANN-Quintic functions for calculating germination percentages (grass suitability).

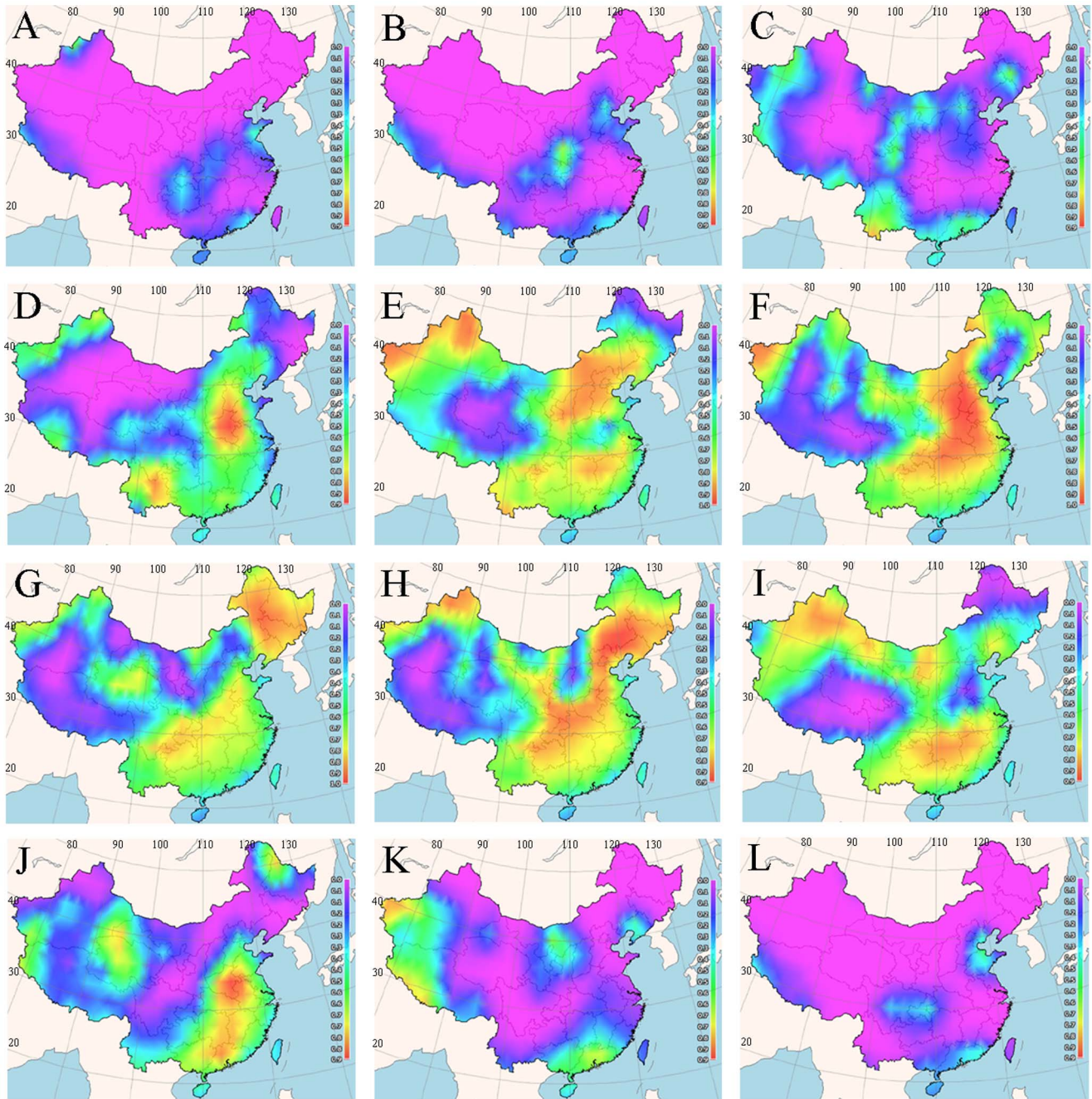


Figure 5. Maps of monthly germination suitability for 'Princess VII' in different regions of China; (A-L) January–December.
doi:10.1371/journal.pone.0082413.g005

Supporting Information

Table S1 Cumulative seed germination of amount *C. dactylon* at different days in 36 temperature regimes (50 seeds in total).
(XLS)

Table S2 Cumulative seed germination amount of *Savannah* at different days in 36 temperature regimes (50 seeds in total).
(XLS)

Table S3 Cumulative seed germination amount of *Princess VII* at different days in 36 temperature regimes (50 seeds in total).
(XLS)

Acknowledgments

We are grateful to Xi Tang and Meixia Ruan for their kind assistance during seed germination tests. Thanks are also due to Dr Jiang-Feng Guo (Agricultural Technology Extension Station of Qingfeng County, Henan Province, China) for providing the FreeMicaps software and for his kind guidance on software application.

Author Contributions

Conceived and designed the experiments: HL EP. Performed the experiments: EP. Analyzed the data: EP. Contributed reagents/materials/analysis tools: HL EP. Wrote the paper: EP HL LD SN NM.

References

- Farsani TM, Etemadi N, Sayed-Tabatabaei BE, Talebi M (2012) Assessment of Genetic Diversity of Bermudagrass (*Cynodon dactylon*) Using ISSR Markers. *Int J Mol Sci* 13: 383–392.
- Huang CQ, Huang DY, Zhang YF, Liu GD (2010) Genetic analysis for 57 accessions of *Cynodon dactylon* from 17 countries in 5 continents by SRAP markers. *Trop Grasslands* 44: 274–281.
- Caglar BK, Satar S, Elbeaino T (2013) Detection and Molecular Characterization of Bermuda Grass (*Cynodon dactylon*) White Leaf Phytoplasma from Turkey. *Int J Agric Biol* 15: 90–94.
- Hameed M, Ashraf M, Naz N, Nawaz T, Batool R, et al. (2013) Anatomical Adaptations of *Cynodon Dactylon* (L.) Pers. From the Salt Range (Pakistan) to Salinity Stress. II. Leaf Anatomy. *Pak J Bot* 45: 133–142.
- Heshmati GA, Pesaraki M (2011) Threshold Model in Studies of Ecological Recovery in Bermudagrass (*Cynodon Dactylon* L.) under Nutrient Stress Conditions. *J Plant Nutr* 34: 2183–2192.
- Adebiyi FM, Ayeni OA (2010) Evaluation of Phytoaccumulation of Selected Metals from Petroleum Products Impacted-Soils by *Cynodon dactylon* Plants Using AAS/AES Analytical Techniques. *Anal Lett* 43: 1879–1888.
- Castillo AM, Tercero TM, Davis JM (2009) Biocalculation of lead and cadmium in *Bouteloua curtipendula* and *Cynodon dactylon*. *Abstr Pap Am Chem S* 237.
- Gayathri U, Venkatraman BR, Arivoli S (2011) Removal of Copper (II) Ions from Aqueous Solutions by Adsorption with Low Cost Acid Activated *Cynodon Dactylon* Carbon. *E-J Chem* 8: S377–S391.
- Wang YB, Zhang L, Yao J, Huang YJ, Yan M (2009) Accumulation and Resistance to Copper of Two Biotypes of *Cynodon dactylon*. *B Environ Contam Tox* 82: 454–459.
- Wu FY, Bi YL, Leung HM, Ye ZH, Lin XG, et al. (2010) Accumulation of As, Pb, Zn, Cd and Cu and arbuscular mycorrhizal status in populations of *Cynodon dactylon* grown on metal-contaminated soils. *Appl Soil Ecol* 44: 213–218.
- Dhoke V, Mishra A, Vohra R, Ghosh R, Kadam VJ (2008) Pharmacological evaluation for anti-ulcer effect of *Cynodon dactylon* pers. Against gastric ulcers in rats. *Indian J Pharmacol* 40: 69–70.
- Garg VK, Paliwal SK (2011) Anti-Inflammatory Activity of Aqueous Extract of *Cynodon dactylon*. *Int J Pharmacol* 7: 370–375.
- Arjunan N, Murugan K, Madhivazhagan P, Kovendan K, Prasannakumar K, et al. (2012) Mosquitocidal and water purification properties of *Cynodon dactylon*, *Aloe vera*, *Hemidesmus indicus* and *Coleus amboinicus* leaf extracts against the mosquito vectors. *Parasitol Res* 110: 1435–1443.
- Balasubramanian G, Sarathi M, Venkatesan C, Thomas J, Hameed ASS (2008) Oral administration of antiviral plant extract of *Cynodon dactylon* on a large scale production against White spot syndrome virus (WSSV) in *Penaeus monodon*. *Aquaculture* 279: 2–5.
- Kaleswaran B, Ilaivelil S, Ravikumar S (2011) Dietary supplementation with *Cynodon dactylon* (L.) enhances innate immunity and disease resistance of Indian major carp, Cat la catla (Ham.). *Fish Shellfish Immun* 31: 953–962.
- Mangathayaru K, Umadevi M, Reddy CU (2009) Evaluation of the immunomodulatory and DNA protective activities of the shoots of *Cynodon dactylon*. *J Ethnopharmacol* 123: 181–184.
- Babu DSR, Neeharika V, Pallavi V, Reddy BM (2009) Antidiarrheal activity of *Cynodon Dactylon*. *pers. Pharmacogn Mag* 5: 23–27.
- Rad AK, Hadjzadeh MAR, Rajaei Z, Mohammadian N, Valiollahi S, et al. (2011) The Beneficial Effect of *Cynodon Dactylon* Fractions on Ethylene Glycol-Induced Kidney Calculi in Rats. *Urol J* 8: 179–184.
- Pal D (2008) Evaluation of CNS activities of aerial parts of *Cynodon dactylon* Pers. in mice. *Acta Pol Pharm* 65: 37–43.
- Pal DK, Kumar M, Chakraborty P, Kumar S (2008) Evaluation of the antioxidant activity of aerial parts of *Cynodon dactylon*. *Asian J Chem* 20: 2479–2481.
- Devi KMS, Annapoorani S, Ashokkumar K (2011) Hepatic antioxidative potential of ethyl acetate fraction of *Cynodon dactylon* in Balb/c mice. *J Med Plants Res* 5: 992–996.
- Rai DK, Sharma RK, Rai PK, Watal G, Sharma B (2011) Role of aqueous extract of *Cynodon dactylon* in prevention of carbofuran-induced oxidative stress and acetylcholinesterase inhibition rat brain. *Cell Mol Biol* 57: 135–142.
- Sindhu G, Ratheesh M, Shyni GL, Helen A (2009) Inhibitory effects of *Cynodon dactylon* L. on inflammation and oxidative stress in adjuvant treated rats. *Immunopharm Immunot* 31: 647–653.
- Garcia-Mozo H, Galan C, Belmonte J, Bermejo D, Candau P, et al. (2009) Predicting the start and peak dates of the Poaceae pollen season in Spain using process-based models. *Agr Forest Meteorol* 149: 256–262.
- Recio M, Docampo S, Garcia-Sanchez J, Trigo MM, Melgar M, et al. (2010) Influence of temperature, rainfall and wind trends on grass pollination in Malaga (western Mediterranean coast). *Agr Forest Meteorol* 150: 931–940.
- van Oort PAJ, Zhang TY, de Vries ME, Heinemann AB, Meinke H (2011) Correlation between temperature and phenology prediction error in rice (*Oryza sativa* L.). *Agr Forest Meteorol* 151: 1545–1555.
- Bradford KJ (2002) Applications of hydrothermal time to quantifying and modeling seed germination and dormancy. *Weed Sci* 50: 248–260.
- Hardegee S, Van Vactor S (1999) Predicting germination response of four cool-season range grasses to field-variable temperature regimes. *Environ Exp Bot* 41: 209–217.
- Hardegee SP, Van Vactor SS, Pierson FB, Palmquist DE (1999) Predicting variable-temperature response of non-dormant seeds from constant-temperature germination data. *Journal of Range Management*: 83–91.
- Hardegee SP (2006) Predicting germination response to temperature. I. Cardinal-temperature models and subpopulation-specific regression. *Annals of Botany* 97: 1115–1125.
- Hardegee SP (2006) Predicting germination response to temperature. III. Model validation under field-variable temperature conditions. *Ann Bot-London* 98: 827–834.
- Hardegee SP, Winstral AH (2006) Predicting germination response to temperature. II. Three-dimensional regression, statistical gridding and iterative-probit optimization using measured and interpolated-subpopulation data. *Ann Bot-London* 98: 403–410.
- Roberts E (1988) Temperature and seed germination. *Symposia of the Society for Experimental Biology*. 109.
- Thompson K, Grime J, Mason G (1977) Seed germination in response to diurnal fluctuations of temperature. *Nature* 267: 147–149.
- Vandelook F, Van Assche JA (2008) Temperature requirements for seed germination and seedling development determine timing of seedling emergence of three monocotyledonous temperate forest spring geophytes. *Ann Bot-London* 102: 865–875.
- Lu H, Shen J, Jin X, Hannaway DB, Daly C, et al. (2008) Determining optimal seeding times for tall fescue using germination studies and spatial climate analysis. *Agr Forest Meteorol* 148: 931–941.
- Daly C, Gibson WP, Taylor GH, Johnson GL, Pasteris P (2002) A knowledge-based approach to the statistical mapping of climate. *Clim Res* 22: 99–113.
- Gazola S, Scapim CA, Guedes TA, Braccini AdL (2011) Nonlinear proposal modeling of seed germination performance of hybrid corn seeds. *Ciência Rural* 41: 551–556.
- Onofri A, Carbonell E, PIEPHO HP, Mortimer A, Cousens R (2010) Current statistical issues in Weed Research. *Weed Res* 50: 5–24.
- Shetty N, Olesen MH, Gislum R, Deleuran LC, Boelt B (2012) Use of partial least squares discriminant analysis on visible-near infrared multispectral image data to examine germination ability and germ length in spinach seeds. *J Chemometr* 26: 462–466.
- Shen J, Xu L, Jin X, Chen J, Lu H (2008) Effect of temperature regime on germination of seed of perennial ryegrass (*Lolium perenne*). *Grass Forage Sci* 63: 249–256.
- Rasul G, Humphreys GD, Wu J, Brülé-Babel A, Fofana B, et al. (2012) Evaluation of preharvest sprouting traits in a collection of spring wheat germplasm using genotype and genotype × environment interaction model. *Plant Breeding* 131: 244–251.
- Falamaki A (2013) Artificial neural network application for predicting soil distribution coefficient of nickel. *J Environ Radioact* 115: 6–12.
- Rivera-Reyes J, Peraza-Luna F, Serratos-Arévalo J, Posos-Ponce P, Guzmán-Maldonado S, et al. (2009) Effect of nitrogen and phosphorus fertilization on phytic acid concentration and vigor of oat seed (var. Saia) in Mexico. *Phyton (Buenos Aires)* 78: 37–42.
- Evrendilek F (2013) Quantifying biosphere-atmosphere exchange of CO₂ using eddy covariance, wavelet denoising, neural networks, and multiple regression models. *Agr Forest Meteorol* 171: 1–8.
- Catalogna M, Cohen E, Fishman S, Halpern Z, Nevo U, et al. (2012) Artificial neural networks based controller for glucose monitoring during clamp test. *PLoS one* 7: e44587.
- Akdemir B, Oran B, Gunes S, Karaaslan S (2009) Prediction of aortic diameter values in healthy Turkish infants, children, and adolescents by using artificial neural network. *J Med Syst* 33: 379–388.
- Alam M, Briggs A (2011) DA1 Artificial Neural Network Meta-Models in Cost-Effectiveness analysis of intensive Blood-Glucose Control: A Case Study Applied to the UK prospective Diabetes Study (UKPDS) Individual Patient outcome Simulation Model. *Value Health* 14: A234–A235.
- Adamowski J, Chan HF, Prasher SO, Ozga-Zielinski B, Sliusarieva A (2012) Comparison of multiple linear and nonlinear regression, autoregressive integrated moving average, artificial neural network, and wavelet artificial neural network methods for urban water demand forecasting in Montreal, Canada. *Water Resour Res* 48.

50. Alvarez R, Steinbach H, Bono A (2011) An artificial neural network approach for predicting soil carbon budget in agroecosystems. *Soil Sci Soc Am J* 75: 965–975.
51. Larsen PE, Field D, Gilbert JA (2012) Predicting bacterial community assemblages using an artificial neural network approach. *Nat Methods* 9: 621–625.
52. Ahmadi H, Golian A (2010) Growth analysis of chickens fed diets varying in the percentage of metabolizable energy provided by protein, fat, and carbohydrate through artificial neural network. *Poultry Sci* 89: 173–179.
53. Poonnoy P, Tansakul A, Chimman M (2007) Artificial Neural Network Modeling for Temperature and Moisture Content Prediction in Tomato Slices Undergoing Microwave-Vacuum Drying. *J Food Sci* 72: E042–E047.
54. Torrecilla JS, Mena ML, Yáñez-Sedeño P, García J (2007) Quantification of phenolic compounds in olive oil mill wastewater by artificial neural network/laccase biosensor. *J Agr Food Chem* 55: 7418–7426.
55. Zheng H, Jiang L, Lou H, Hu Y, Kong X, et al. (2010) Application of artificial neural network (ANN) and partial least-squares regression (PLSR) to predict the changes of anthocyanins, ascorbic acid, Total phenols, flavonoids, and antioxidant activity during storage of red bayberry juice based on fractal analysis and red, green, and blue (RGB) intensity values. *J Agr Food Chem* 59: 592–600.
56. Zhao X, Xua K, Shia H, Chengb J, Mac J, et al. (2013) Application of the back-error propagation artificial neural network (BPANN) on genetic variants in the PPAR- γ and RXR- α gene and risk of metabolic syndrome in a Chinese Han population. *J Biomed Res* 27. doi:10.7555/JBR.27.20120061.
57. Karnin ED (1990) A simple procedure for pruning back-propagation trained neural networks. *Neural Networks, IEEE Transactions on* 1: 239–242.
58. Chang W, Bosworth B, Carter GC (1993) Empirical results of using back-propagation neural networks to separate single echoes from multiple echoes. *Neural Networks, IEEE Transactions on* 4: 993–995.
59. Pan Y, Jiang J, Wang Z (2007) Quantitative structure–property relationship studies for predicting flash points of alkanes using group bond contribution method with back-propagation neural network. *J Hazard Mater* 147: 424–430.
60. Omelka M, Salibián-Barrera M (2010) Uniform asymptotics for S-and MM-regression estimators. *Ann I Stat Math* 62: 897–927.
61. Hampel F, Hennig C, Ronchetti E (2011) A smoothing principle for the Huber and other location M-estimators. *Comput Stat and An* 55: 324–337.
62. Ji J (2012) Robust inversion using biweight norm and its application to seismic inversion. *Explor Geophys* 43: 70–76.
63. Maddahi A, Shahriari H, Shokouhi AH (2011) A robust (X)over-bar control chart based on M-estimators in presence of outliers. *Int J Adv Manuf Tech* 56: 711–719.
64. Barnhart B, Eichinger W, Prueger J (2012) Introducing an Ogive method for discontinuous data. *Agr Forest Meteorol* 162: 58–62.
65. Hema M, Srinivasan K (2011) Artificial neural network and multiple regression model for nickel (II) adsorption on powdered activated carbons. *Journal of Environmental Science & Engineering* 53: 237.
66. Yun J, Mackenzie M, Rathee S, Robinson D, Fallone B (2012) An artificial neural network (ANN)-based lung-tumor motion predictor for intrafractional MR tumor tracking. *Med Phys* 39: 4423.
67. Modi Y, De Beer D, Agrawal S (2011) Physical modelling of terrain directly from surfer grid and ARC/INFO ASCII data formats. *S Afr J Ind Eng* 23: 230–241.